Carbohydrate Polymers 94 (2013) 46–55

Contents lists available at SciVerse ScienceDirect

Carbohydrate Polymers

journal homepage: www.elsevier.com/locate/carbpol

Fractionation and structural characterization of LiCl–DMSO soluble hemicelluloses from tomato

Carole Assor, Bernard Quemener, Jacqueline Vigouroux, Marc Lahaye*

INRA, UR 1268 Biopolymers, Interactions and Assemblies, rue de la Géraudière, F-44316 Nantes, France

ARTICLE INFO

Article history:
Received 27 September 2012
Received in revised form
21 December 2012
Accepted 1 January 2013
Available online 9 January 2013

Keywords:
Cell wall
Solanum lycopersicom
Acetyl esterified hemicelluloses
Xyloglucans
Galactoglucomannans
Glucuronoxylans
MALDI-TOF MS

ABSTRACT

To prepare and explore the structure of native hemicellulose from tomato, extraction of the natively acetylated polysaccharides was achieved from partially depectinated cell walls by DMSO doped with LiCl. DEAE anion exchange chromatography of the LiCl–DMSO extract allowed the removal of residual acidic pectin and the isolation of acetylated glucuronoxylan. The hemicellulose neutral fraction from the anion exchanger was fractionated by size exclusion chromatography into xyloglucan (XyG) and galactoglucomannan (GgM) either as single major constituents or as mixtures of both. Residual hemicellulose in the cell wall was extracted by 4.0 M and not 1.0 M KOH. The fine structure of all LiCl–DMSO fractions and alkali extracts was assessed by coupling β-glucanase, β-mannanase and β-xylanase enzymatic degradations to the analysis of the resulting fragments by HPAEC and MALDI-TOF mass spectrometry. This approach revealed substitutions in part of the GgM fractions by pentose residues, presumably arabinose and/or xylose occurring in highly substituted block domains. It also demonstrated a different glucanase hydrolysis profile from 4.0 M KOH compared to LiCl–DMSO soluble fractions. The present extraction and purification scheme allow the recovery of several populations of acetylated hemicellulose families which emphasize the structural diversity and complexity of these polysaccharides.

1. Introduction

Tomato is a widely used model to study biological and qualitative aspects of fleshy fruits (Klee & Giovannoni, 2011). Among qualitative aspects, texture variation is a major concern driving consumer choice (Causse et al., 2010). Fleshy fruit texture results from a combination of several factors at different scales, such as cuticle structure, turgor pressure and tissues cellular features, but it has extensively been studied with regard to cell wall polysaccharide disassembly processes owing to the fact that softening during ripening involves cell–cell debonding and cell wall swelling (Abbott & Lu, 1996; Brummell, 2006; Guillon et al., 2008; Saladie et al., 2007; Waldron, Park, & Smith, 2003). Besides homogalacturonan and rhamnogalacturonan pectic polysaccharides, tomato cell walls comprise xyloglucan (XyG), galactoglucomannan (GgM) and minor amounts of glucuronoxylan (GuX) hemicelluloses (Brummell, 2006; Prakash et al., 2012; Seymour, Colquhoun, Dupont, Parsley, & Selvendran, 1990). Pectin is involved in cell–cell interaction and wall porosity and is heavily modified during ripening. In contrast hemicelluloses, which interact with cellulose to modulate the load-bearing contribution of the cellulose microfibrills to the wall, do not appear to be markedly degraded during tomato ripening (Brummell, 2006; Cosgrove & Jarvis, 2012). Hemicelluloses and their interactions appear determinant in fruit texture. To date, of the tomato mutants down- or up-regulated for the expression of the major cell wall disassembly enzymes and proteins, only those affecting XyG interactions with cellulose or in xyloglucan structures were successful in impacting fruit softening (Brummell et al., 1999; Kalamaki et al., 2003; Miedes, Herbers, Sonnewald, & Lorences, 2010; Powell, Kalamaki, Kurien, Gurrieri, & Bennett, 2003).

Xyloglucan exists in the cell wall as different molecular populations (Pauly, Albersheim, Darvill, & York, 1999). A minor fraction intertwined within the cellulose microfibrills and of limited access to enzymes controls cell wall mechanical characteristics (Park & Cosgrove, 2012). In tomato, xyloglucan (XyG) consists of a backbone of β-(1 → 4)-linked D-glucose (noted **G**; Fry et al., 1993) substituted with α-(1 → 6)-D-xylose (noted **X**) more or less extended by one β-D-galactosyl (noted **L**), one α-L-arabinosyl (noted **S**) residue or by the disaccharide β-L-arabinosyl (1 → 3) α-L-arabinoside (noted **T**) linked on xylose O-2 (Jia, Cash, Darvill, & York, 2005). Side chain distribution in tomato XyG leads to glucanase degradation products generally ending by two consecutive **G** units at the reducing end (**XXGG**-type) and contrast to the more general **XXXG**-type of most other plants (Vincken, York, Beldman, & Voragen, 1997). Tomato XyG can further be substituted by acetyl ester groups on O-6 of

* Corresponding author.
E-mail addresses: cassor@nantes.inra.fr (C. Assor), lahaye@nantes.inra.fr (M. Lahaye).

0144-8617/$ – see front matter © 2013 Elsevier Ltd. All rights reserved.
http://dx.doi.org/10.1016/j.carbpol.2013.01.001

unramified glucose residues, on O-6 of terminal galactose and on O-5 of terminal arabinose residues in the side chains (Jia et al., 2005).

XyG side chains structure is reshuffled during plant development according to organ (Obel et al., 2009; Pauly et al., 2001) through specific cell wall glycohydrolases and transglycosylases (Frankova & Fry, 2012; Gunl et al., 2011; Sampedro et al., 2012). In tomato, the fine structure of the enzyme accessible XyG domains varies with genetics and is modified by ripening (Lahaye, Quemener, Causse, & Seymour, 2012). These changes suggest that more subtle remodeling of these polysaccharides may be involved in the cell wall loosening process. Such modifications likely impact XyG macromolecular re-assembly mediated by xyloglucan endotransglycosylase/hydrolase (XTH) activities (Eklof & Brumer, 2010) and hydrogen bonding abilities (de Freitas, Busato, Mitchell, & Silveira, 2011; Lopez et al., 2010) but the exact functions of these fine structural modifications remain to be identified.

Galactoglucomannan (GgM) has been reported in Solanaceae primary walls (Eda, Akiyama, & Kato, 1985; Eda et al., 1984; Sims, Craik, & Bacic, 1997) and recently Prakash et al. (2012) isolated galactoglucomannan from tomato fruit. It is extracted by DMSO and 4 M KOH and is linked to glucuronoxylan. The DMSO fraction is richer in xylan and appeared more branched than the KOH soluble fraction. The overall structure of these fractions is not affected by ripening. In the closely related species, *Nicotania tabacum* and *N. plumbagnifolia*, GgM is predominantly composed of alternating 1,4-linked β-D-glucose and β-D-mannose backbone branched at O-6 of the mannose residues by α-D-galactopyranosyl or 2-O-β-D-galactopyranosyl-α-D-galactopyranosyl side-chains. It contains small amounts of terminal arabinose and xylose and is partially acetyl esterified (Eda et al., 1985; Sims et al., 1997). Like XyG, the fine structure of the enzyme accessible tomato GgM is affected by ripening and genetics (Lahaye et al., 2012). The exact function of GgM in the primary cell wall is unclear. It is located at cell surface and appears important for cell adhesion in tomato parenchyma (Ordaz-Ortiz, Marcus, & Knox, 2009). It is depolymerized in vitro by the tomato mannan endotransglycosylase/hydrolyase (MTH) but not in vivo, likely due to dominating transglycosylase activity even during ripening (Prakash et al., 2012; Schröder, Atkinson, & Redgwell, 2009).

Although quantitatively minor in dicots primary walls, glucuronoxylans have also been isolated from other Solanaceae by alkaline extraction of tissue or from cell culture medium and DEAE-anion exchange chromatography (Akiyama, Eda, & Kato, 1984; Eda, Watanabe, & Kato, 1977). It has also been isolated as glucuronoarabinoxylan from the primary wall of Acer cells in culture (Darvill, McNeil, Darvill, & Albersheim, 1980) though its function in cell walls is unclear. It has been located in cell walls lining intercellular spaces in tomato which suggest a role in cell adhesion (Ordaz-Ortiz et al., 2009).

Further improvement of fleshy fruit texture management is expected to benefit from more detailed mechanistic studies of the fruit biochemistry and biophysic using simplified systems, such as cell wall models (Chanliaud, de Silva, Strongitharm, Jeronimidis, & Gidley, 2004; Cybulska et al., 2010; Dammström, Salmén, & Gatenholm, 2005; Tokoh, Takabe, Sugiyama, & Fujita, 2002). They were proven helpful to develop our understanding on relationships between polysaccharides structures on cell wall assembly and mechanical characteristics including the role of enzymes and expansin on these assemblies. To further explore the function of hemicellulose using cell wall models, better defined polysaccharides are required. Chemo-enzymatic synthesis methods are developed to tailor XyG with specific structural domains (Lopez, Fort, Bizot, Buleon, & Driguez, 2012; Spadiut et al., 2011), but extraction and purification of hemicelluloses from plants remain a mean of exploring and accessing at the wide structural diversity existing in Nature. To this goal, this work focuses on the preparation and characterization of representative naturally acetylated hemicellulose fractions from tomato. A non basic polar aprotic solvent of hemicelluloses, DMSO (Hagglund, Lindberg, & McPherson, 1956) doped with LiCl (Petruš, Gray, & BeMiller, 1995) was used instead of the classical alkali NaOH or KOH solutions. The fine structure of purified XyG, GgM and GuX fractions obtained after anion exchange and size exclusion chromatographies was assessed by coupling endo-(1 → 4)-β-D-glucanase, mannanase and xylanase enzymatic degradations to the analysis of the resulting fragments by HPAEC and by matrix-assisted laser desorption ionization-time of flight mass spectrometry (MALDI-TOF-MS).

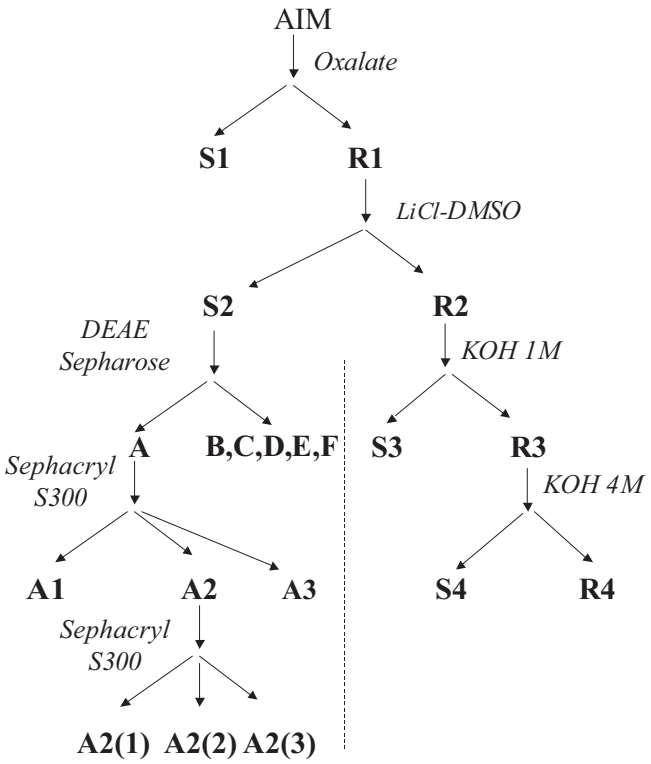

Fig. 1. Hemicellulose extraction and fractionation flow diagram from alcohol insoluble cell wall material (AIM) of green tomato pericarp tissue.

2. Materials and methods

2.1. Cell wall material preparation

Cell wall material was prepared as an alcohol insoluble material (AIM). Pericarp tissue (internal and external) of 20 kg of mature green tomato (var. Levovil) were peeled, cut and boiled in ethanol 96% (solid/liquid ratio: 1/3, w/v) for 20 min and recovered on a nylon cloth (90 μm). The pieces of flesh were washed repeatedly with 72% ethanol (solid/liquid ratio as above, 5 times for 4 h) until the ethanol extract was free of sugar (Dubois, Gilles, Hamilton, Rebers, & Smith, 1956) and finally with 96% ethanol and acetone before drying in an oven at 40 °C.

2.2. Sequential extraction of cell wall polysaccharides

The sequential extraction procedure used is shown in Fig. 1. AIM (16.5 g) pectin was extracted with 500 mL of a 2.5% (v/v) ammonium oxalate solution (0.2 M) in water brought to pH 4.6 with oxalic acid (Koubala et al., 2008). Extraction was carried out at 40 °C for 30 min and then at 85 °C for 30 min with stirring. The residual AIM

was extracted as above twice more (85 °C, 30 min). Each time the solid (**R1**) and liquid (**S1**) fractions were recovered by filtration on sintered glass (16–40 μm).

The residue after oxalate extraction (**R1**) was washed with deionised water until the conductimetry of the wash reached less than 20 $\mu S\,cm^{-1}$. Then, **R1** was washed twice with DMSO at 20 °C (1 g dry weight for 40 mL of DMSO, 30 min), centrifuged 10 min at 12,600 × *g* and filtered on sintered glass (40–100 μm).

Hemicelluloses were extracted from **R1** by 8.4% LiCl–DMSO (1 g dry weight for 200 mL) at 100 °C during 5 h under continuous agitation and under N_2 (Flores, Stortz, & Cerezo, 2000). The suspension was filtered and centrifuged (20 min, 20 °C, 9000 × *g*). The pellet (**R2**) was washed with 200 mL of DMSO, filtered (40–100 μm), centrifuged as above and kept at 4 °C. The DMSO extracts were pooled (**S2**) and evaporated to dryness at 60 °C under vacuum. The dry extract was dissolved with 500 mL of deionised water and precipitated with 2 L of cold 96.2% ethanol (4 °C) under stirring and left to decant overnight at 4 °C. The precipitate was recovered by centrifugation (10 min, 12,600 × *g*, 10 °C), washed with ethanol 96% and dried with acetone.

The LiCl–DMSO residue (**R2**) was washed with deionised water. Remaining hemicelluloses in **R2** (1 g dry weight) were extracted by KOH (1 M, 400 mL) for 17 h at room temperature with stirring in presence of $NaBH_4$ (0.03 $g\,L^{-1}$) (Carpita, 1984). The suspension was centrifuged (9000 × *g*, 20 min) and the supernatant filtered (40–100 μm). **R2** was extracted once more for 1 h in the same conditions. The two extracts were pooled, neutralized with cold acetic acid, dialyzed (MWCO 6000–8000) and freeze-dried (**S3**). The residue (**R3**) was submitted to a 4 M KOH extraction following the same protocol, was washed with 0.1 M acetic acid and with deionised water and freeze-dried (**R4**). The corresponding extracts (**S4**) were treated as **S3**.

2.3. Chemical cell wall composition

Identification and quantification of cell wall neutral sugars were performed by gas–liquid chromatography (GC) after sulfuric acid degradation (Hoebler, Barry, David, & Delort-Laval, 1989). AIM was dispersed in 13 M sulfuric acid for 30 min at 25 °C and then hydrolyzed in 1 M sulfuric acid (2 h, 100 °C). Sugars were converted to alditol acetates (Blakeney, Harris, Henry, & Stone, 1983) and chromatographed on a DB 225 capillary column (J&W Scientific, Folsorn, CA, USA; temperature 205 °C, carrier gas H_2). Standard sugars solution and inositol as internal standard were used for calibration. Uronic acids in hydrolyzates were quantified using the metahydroxydiphenyl colorimetric acid method (Blumenkrantz & Asboe-Hansen, 1973). Contaminating glucose from residual starch in the AIM and in the LiCl–DMSO extract was measured after amylolysis (McCleary, Gibson, & Mugford, 1997) by HPAEC (CarboPac PA1 analytical column, 250 mm × 4 mm, Dionex). Each analysis is a mean of two measures. The error was less than 0.4%.

Soluble protein were measured by the Bradford colorimetric method with the Bio-Rad reagent and using BSA as standard (Bradford, 1976). Insoluble protein were measured by the Kjeldahl method (N X 6.25).

Acetic acid content was measured enzymatically (BioSenTec, Toulouse, France) after saponification of 5 mg samples in 1 mL NaOH 0.50 M for 1 h at room temperature followed by neutralization with HCl 1 M (0.5 mL).

2.4. Fractionation of hemicelluloses

2.4.1. DEAE anion exchange chromatography

Anion exchange chromatography was performed on a DEAE Sepharose Fast Flow column (GE Healthcare, 50 mm × 150 mm) equilibrated in 50 mM sodium acetate buffer pH 4.5. The dialyzed and freeze-dried LiCl–DMSO extract (**S2**) was dissolved in the same buffer at a final concentration of 20.9 $g\,L^{-1}$ and applied to the anion-exchanger. Elution of neutral polysaccharides (fraction **A**) was realized by 960 mL of 50 mM sodium acetate buffer (pH 4.5) at a flow rate of 2 mL min^{-1}. A gradient (total volume 1.8 L) from 0 to 100% of NaCl 1 M in the same buffer was then applied to elute acidic polysaccharide fractions. Collected fractions were analyzed for their total sugars content by colorimetry (Tollier & Robin, 1979) and fractions corresponding to eluted peaks were pooled, dialyzed and freeze-dried (fractions **B**–**F**).

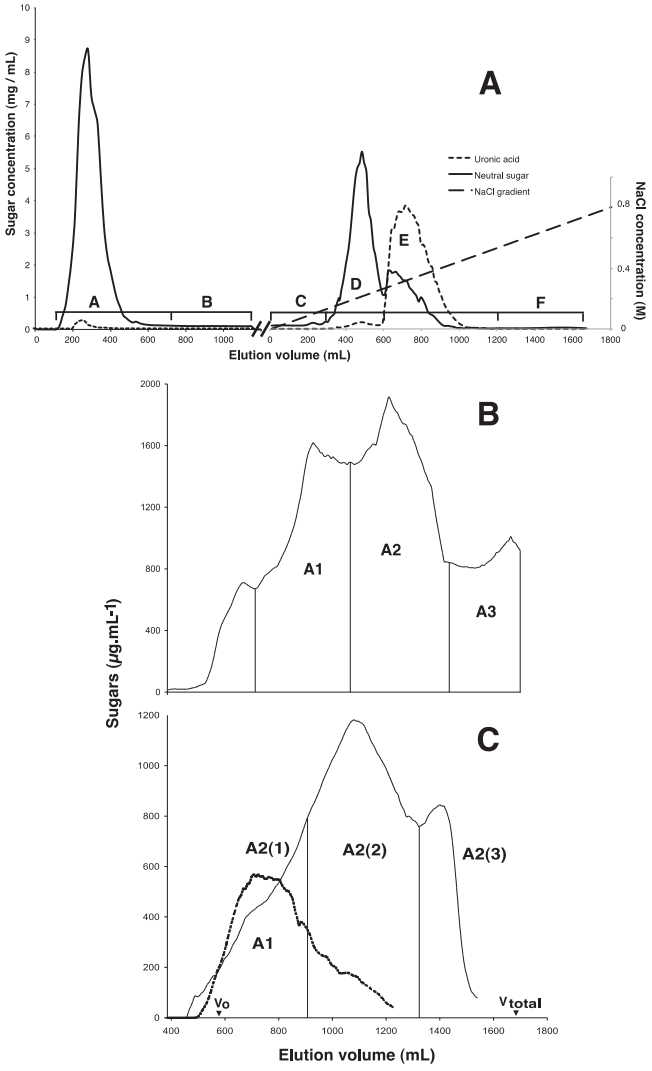

Fig. 2. DEAE-Sepahrose (A) and Sephacryl S300 gel permeation (B) chromatographies of fraction **S2** recovered after LiCl–DMSO extraction of AIM; (C) second Sephacryl S300 gel permeation chromatography of fraction **A2** (recovered from the first gel filtration).

2.4.2. Size exclusion chromatography

Fraction **A** (1.42 g in 60 mL of 50 mM sodium nitrate) from the anion exchanger was applied on a Sephacryl S300 column (GE Healthcare, 50 mm × 870 mm) and was eluted in the same buffer at a flow rate of 100 mL h^{-1}. Fractions collected were analyzed for their total sugar content by colorimetry (Tollier & Robin, 1979) and fractions corresponding to eluted peaks (fractions **A1**, **A2**, **A3**,) were pooled, dialyzed and freeze-dried. Fraction **A1** and **A2** were re-fractionnated on the same column Fraction A2 yielded **A2 (1), A2 (2)** and **A2 (3)** while **A1** was eluted as a single peak

Table 1
Yield and chemical composition (standard deviation) on the percent dry weight basis of the AIM and subsequent fractions (residues (**R**) and solubles (**S**)) obtained from the different extractions (oxalate (**R1**, **S1**), LiCl–DMSO (**R2**, **S2**) and KOH (**R3**, **S3**, **R4**, **S4**)) and from the DEAE anion exchange (**A**, **B**, **C**, **D**, **E**, **F**) and gel permeation fractionation (**A1**, **A2**, **A3 and A2(1)**, **A2(2)**, **A2(3)**) chromatographies.

Fraction	Yield (AIM dw%)	Sugar								Acetyl ester[c] (dw%)	Protein (dw%)
		Rha (dw%)	Ara (dw%)	Xyl (dw%)	Man (dw%)	Gal (dw%)	Glc (dw%)	UA (dw%)	Total sugar		
AIM			3.8 (0.1)	3.6 (0.3)	4.1 (0.5)	9.4 (0.6)	29.6 (4.4)	23.0 (0.9)	74.2 (5.9)	1.7	
S1	15.0	1.1 (0.1)	2.5 (0.2)		2.1 (0.1)	6.1 (0.4)	1.9 (0.0)	57.7 (0.1)	71.8 (1.0)	0.7	8.7
R1	85.0		3.9 (0.0)	4.2 (0.2)	4.6 (0.0)	10.0 (0.1)	39.0 (0.2)	12.7 (0.0)	75.0 (0.5)	1.7	
S2	16.0		2.5 (0.1)	10.3 (0.3)	6.7 (0.5)	7.4 (0.3)	11.6 (0.7)	22.8 (0.0)	61.8 (2.1)	3.9	
R2	60.0		7.7 (0.0)	2.4 (0.0)	1.0 (0.0)	9.7 (0.1)	46.9 (0.6)	7.0 (0.0)	71.3 (0.8)	1.2[d]	
S3[a]	5.0		4.4	1.4		13.5	3.3	3.3	27.5		35.2
S4[a]	6.0		6.9	13.0		16.8	25.8	3.5	67.4		0.9
R4	36.0		2.2 (0.0)	1.1 (0.0)	1.2 (0.0)	6.0 (0.1)	26.3 (1.0)	3.3 (0.0)	40.4 (1.2)		
A	6.0		3.8 (0.0)	11.0 (0.2)	23.5 (0.6)	15.9 (0.7)	43.8 (1.1)	1.6 (0.4)	99.7 (2.6)	4.3	3.0
B[a]	0.1			67.0	2.1	1.7	6.7	4.7	83.1		
C[a]	0.1		1.1	69.0		3.0	5.3	5.8	85.1		
D	2.0		1.5 (0.1)	73.2 (0.9)		6.7 (0.3)		8.3 (0.5)	90.8 (0.42)	5.6	1.6
E	6.0	1.2 (0.2)	3.6 (0.4)	2.1 (0.7)		9.0 (1.0)		76.2 (4.8)	92.1 (0.1)	1.4	1.3
F[a,b]	0.1		2.8	1.1		6.6		8.9	31.2		11.0
A1	0.8		6.0 (0.1)	19.1 (0.2)	7.5 (0.2)	15.3 (0.5)	50.4 (0.3)	2.5 (0.0)	100.8 (1.4)		5.0
A2	2.0		2.1 (0.0)	8.3 (0.0)	30.7 (0.8)	13.7 (0.2)	40.4 (0.9)	1.0 (0.1)	96.2 (1.8)		
A3[a]	1.5	0.3	0.6	2.4	37.2	15.0	30.2	1.8	87.4	4.6	
A2(1)[a]			3.8	12.3	9.4	9.5	35.2	nd[e]	70.2	5.5	
A2(2)[a]			1.2	4.9	29.4	11.3	31.4	nd	78.3	6.3	
A2(3)[a]			0.8	4.9	32.1	12.6	31.3	nd	81.8	6.1	

Rha: rhamnose; Ara: arabinose; Xyl: xylose; Man: mannose; Gal: galactose; Glc: glucose, UA: uronic acid; residues (**R**) and solubles (**S**) from hemicelluloses extraction sequences (Fig. 1).

[a] One sample analyzed.
[b] Contained 11.0% of ribose (%dry weight).
[c] Standard deviation < 0.1.
[d] Likely overestimated due to residual acetate from solvent.
[e] Non determined.

2.5. Structural characterization of hemicelluloses

2.5.1. Enzymatic degradations

Cell wall preparations, extracts, extraction residues and chromatographic fractions were degraded by endo-1,4-β-glucanase, endo-1,4-β-xylanase (M2) from *Trichoderma longibrachiatum* (Megazyme, Bray, Ireland) or endo-1,4-β-mannanase from *Aspergillus niger* (Megazyme) and the oligosaccharides released were analyzed by HPAEC and MALDI-TOF MS. Samples (5 mg) were suspended in 1 mL deionised water containing either 10 U of β-glucanase, or 4.5 U of β-mannanase or 13 U of β-xylanase at 40 °C under slow agitation during 17 h. After enzyme inactivation by boiling 10 min and centrifugation (15,200 × *g*, 10 min at 20 °C), solutions were passed through 0.45 μm filter prior to further HPAEC and MALDI-TOF MS analysis. The commercial source of glucanase was known to be contaminated by endo-β-1,4-D-xylanase activity and was observed to degrade tomato glucomannan and pectic β-1,4-D-galactan (Lahaye et al., 2012).

2.5.2. MALDI-TOF MS

Glucanase, mannanase and xylanase hydrolyzates (10 μL) were mixed with the Super DHB matrix (10 μL; Karas et al., 1993). The matrix was prepared by a mixture (90/10, v/v) of 2,5-dihydroxybenzoic acid (DHB) at 10 mg mL^{-1} in water and 2-hydroxy-5-methoxybenzoic acid at 10 mg mL^{-1} in pure methanol, respectively. Finally 4 μL of the mixture were deposited on the target and left to dry overnight at room temperature. For each hydrolyzate, three replicates were realized.

MALDI-TOF MS analysis was performed in the positive ion mode on a MALDI-TOF/TOF (Autoflex III Smartbeam, Bruker, Germany) equipped with a Yag laser (355 nm). Analyses were carried out in the reflector mode using a laser frequence of 200 Hz and an accelerating voltage of 19 kV. Spectra were recorded in the mass range *m/z* 500–3000. A low mass gate value of *m/z* 500 was selected for analysis in order to avoid saturation of the detector. The instrument was externally calibrated using the monoisotopic masses of main oligosaccharides [M+Na]+ sodium adducts) released from apple xyloglucans after glucanase degradation (**XXG**: 791.263 Da, **XXXG**: 1085.358 Da, **XXFGa1**: 1435.478 Da, **XLFGa1**: 1597.531 Da).

The nomenclature of oligomers released by glucanase followed that of (Fry et al., 1993) for xyloglucans extended to account for acetyl groups noted **a**. Hexose containing oligosaccharides attributed to galactoglucomannans were noted **H**. Pentose

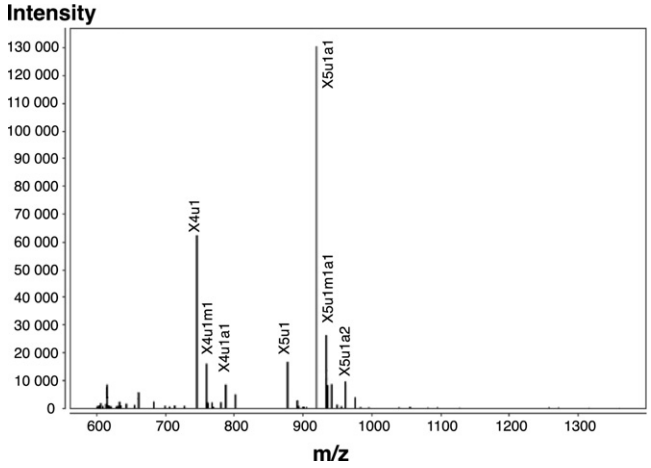

Fig. 3. MALDI-TOF MS spectrum of the β-xylanase degradation products from the **D** fraction recovered after DEAE anion exchange chromatography of the LiCl–DMSO soluble fraction **S2**. The nomenclature is as described in the text.

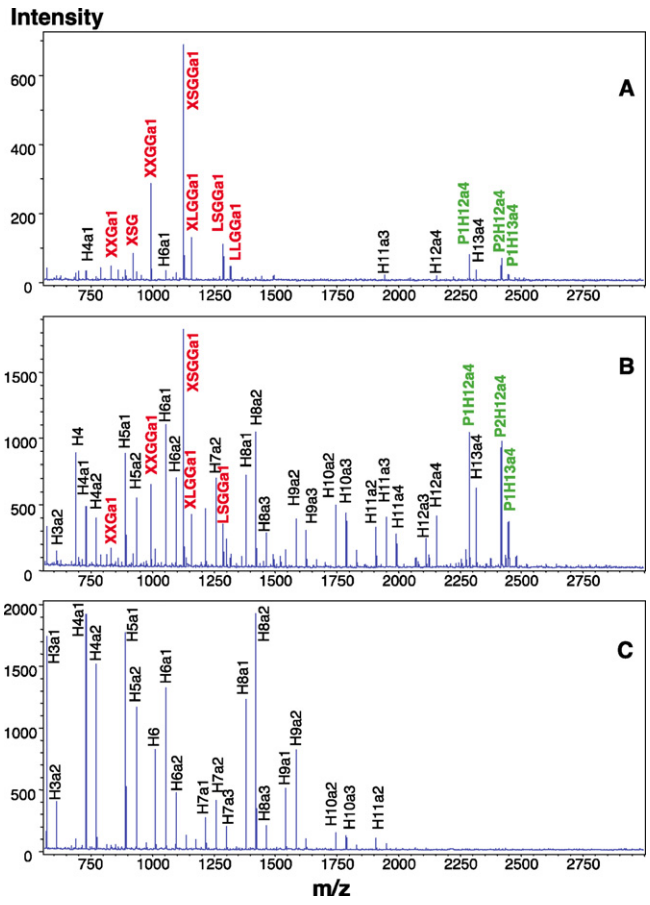

Fig. 4. Mean MALDI-TOF MS spectrum of the β-glucanase degradation products of fractions **A1** (A), **A2** (B) and of mannanase degradation products of **A2** (C). The nomenclature is as described in the text.

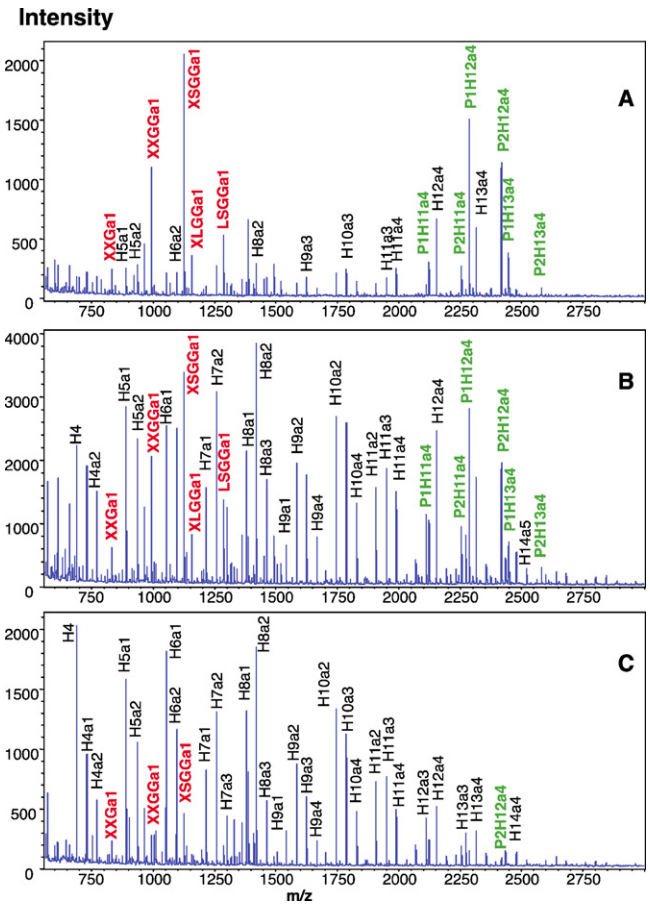

Fig. 5. Mean MALDI-TOF MS spectra of the β-glucanase degradation products of pooled fractions after second Sephacryl S300 fractionation: (A) **A2(1)**, (B) **A2(2)** and (C) **A2(3)**. The nomenclature is as described in the text.

containing oligosaccharides recovered after xylanase degradation were noted **X** otherwise they are noted as **P**. In all oligomer codes, extension with the letter **u**, **m** and **a** refers substitution by an uronic acid, a methyl and acetyl group, respectively. The number following the letter codes denoted the number of building hexosyl units, methyl or acetyl groups in the oligosaccharides (i.e. **H3a1** corresponds to 3 hexosyl units and 1 acetyl group). Reduced oligosaccharides are ended by **ol**.

2.5.3. HPAE-PAD chromatography

Enzymatic digests were monitored by HPAE chromatography using an ICS-3000 pump (Dionex, Sunnyvale, USA) fitted with an AS 3500 auto-sampler (Thermo Separation Products, USA) and an ED 50A electrochemical detector (Dionex, Sunnyvale, USA) working in amperometric mode. After appropriate dilution, an aliquot of 20 μL of the different enzymic digests was injected on an analytical Carbopac PA-200 column (3 mm × 250 mm, Dionex, Sunnyvale, USA) thermostated to 30 °C using the Croco-cil (Cil Cluzeau Info Labo, France) and equipped with a Dionex Carbopac PA-200 guard column (3 mm × 50 mm). Dionex Chromeleon chromatography software was used for controlling the chromatograph and for processing the data. The separation of released oligosaccharides was performed in 100 mM NaOH at 0.45 mL min^{-1} with a linear gradient of sodium acetate from 0 to 150 mM for first 45 min. To elute retained compounds from stationary phase, sodium acetate concentration was set to 300 mM for next 5 min. The column was then re-equilibrated for 25 min with 100 mM NaOH.

3. Results and discussion

The overall extraction and fractionation sequences are presented in Fig. 1. The yield and sugar composition of cell wall preparation and soluble and insoluble fractions are given in Table 1.

3.1. Hemicelluloses extraction, fractionation and composition

The cell wall material, prepared as alcohol insoluble material AIM, was depectinated by oxalate extraction. The oxalate soluble fraction (**S1**) and the insoluble residue (**R1**) represented, respectively, 15 and 85% of the initial AIM dry weight (dw%). **S1**, which total sugar content represented 72%, was mainly composed of uronic acid (58%) and some neutral sugars (galactose: 6%; mannose and glucose: around 2%, and rhamnose: <1%) in agreement with the pectic nature of water and chelator soluble polysaccharides from tomato cell walls (MacDougall, Needs, Rigby, & Ring, 1996; Seymour et al., 1990). Hemicelluloses, cellulose and residual pectic polysaccharides (47% of the AIM uronic acids) were recovered in **R1** which contained 87 and 92% of the AIM arabinose and galactose contents and whole of the mannose, xylose and glucose.

Hemicelluloses are classically extracted with strong alkali solutions which leads to de-esterifications and notably losses of acetyl esters (Fry, 1988). To limit structural changes, hemicelluloses were extracted from the oxalate residue **R1** with a cellulose swelling solvent composed of DMSO containing LiCl (Petruš et al., 1995). This extraction yielded about 16% dry weight (dw) soluble polysaccharides (fraction **S2**) from the starting AIM. It contained 45 and 33% of the **R1** xylose and mannose contents mainly attributed to

Table 2
MALDI-TOF MS ions and deduced structure observed from the glucanase, mannanase and xylanase hydrolysates products of fractions **D**, **A1**, **A2**, **A2(1)**, **A2(2)**, **A2(3)**, **A3**, **S4** and **R4**.

Measured m/z[a]	Structure[b]	Fractions	Measured m/z	Structure	Fractions
569.2	**H3a1**	**A2**, **A3**	1277.3	**LLGG**	**S4**, **R4**
611.2	**H3a2**	**A2**	1289.5	**LSGGa1**	**A1**, **A2(2)**, **A2(3)**, **A3**
629.1	**SG**	**S4**	1301.5	**H7a3**	**A3**
689.3	**H4**	**A2(2)**, **A2(3)**, **A3**, **R4**	1319.5	**LLGGa1**	**A2(2)**, **A3**
731.3	**H4a1**	**A2(2)**, **A2(3)**, **A3**	1331.4	**LSGGa2**	**A2(2)**, **A2(3)**
745.2	**X4u1**	**A2(2)**, **A2(3)**, **D**	1337.4	**H8**	**A3**
759.2	**X4u1m1**	**D**	1379.5	**H8a1**	**A2(2)**, **A2(3)**, **A3**
773.3	**H4a2**	**A2(2)**, **A2(3)**, **A3**	1421.5	**H8a2**	**A2(1)**, **A2(2)**, **A2(3)**, **A3**
787.2	**X4u1a1**	**A2(2)**, **A2(3)**, **D**	1463.5	**H8a3**	**A2(1)**, **A2(2)**, **A2(3)**
791.2	**XXG**	**A3**,**S4**, **R4**	1505.5	**H8a4**	**A3**
801.2	**X4u1m1a1**	**D**	1541.6	**H9a1**	**A2(2)**, **A2(3)**, **A3**
833.3	**XXGa1**	**A1**, **A2**	1583.6	**H9a2**	**A2(1)**, **A2(2)**, **A2(3)**, **A3**
851.3	**H5**	**A3**	1625.6	**H9a3**	**A2(1)**, **A2(2)**, **A2(3)**, **A3**
877.2	**X5u1**	**A2(2)**, **A2(3)**, **D**	1667.6	**H9a4**	**A2(1)**, **A2(2)**, **A2(3)**, **A3**
891.2	**X5u1m1**	**D**	1703.7	**H10a1**	**A2(2)**, **A2(3)**, **A3**
893.4	**H5a1**	**A2**, **A3**	1745.7	**H10a2**	**A2(1)**, **A2(2)**, **A2(3)**,**A3**
919.3	**X5u1a1**	**A2(3)**, **D**	1787.7	**H10a3**	**A2(1)**, **A2(2)**, **A2(3)**,**A3**
923.3	**XSG**	**A1**, **S4**, **R4**	1865.8	**H11a1**	**A3**
933.3	**X5u1m1a1**	**D**	1907.8	**H11a2**	**A2(1)**, **A2(2)**, **A2(3)**, **A3**
935.3	**H5a2**	**A2**, **A3**	1949.8	**H11a3**	**A2(1)**, **A2(2)**, **A2(3)**,**A3**
953.2	**XXGG**	**A3**, **S4**, **R4**	1991.8	**H11a4**	**A3**
961.2	**X5u1a2**	**A2(3)**, **D**	2069.9	**H12a2**	**A2(2)**, **A2(3)**
975.3	**X5u1m1a2**	**D**	2111.9	**H12a3**	**A2(2)**, **A2(3)**
977.3	**H5a3**	**A2**	2124.0	**P1H11a4**	**A2(1)**, **A2(2)**
995.4	**XXGGa1**	**A1**, **A2**, **A2(2)**, **A2(3)**	2153.9	**H12a4**	**A2(1)**, **A2(2)**, **A2(3)**
1009.3	**X6u1**	**A2(2)**, **A2(3)**	2196.0	**H12a5**	**A2(2)**, **A2(3)**
1013.4	**H6**	**A2**, **A3**	2256.1	**P2H11a4**	**A2(1)**, **A2(2)**
1051.3	**X6u1a1**	**A2(2)**, **A2(3)**	2274.1	**H13a3**	**A2(2)**, **A2(3)**
1055.4	**H6a1**	**A2**, **A3**	2286.1	**P1H12a4**	**A1**, **A2(1)**, **A2(2)**
1085.3	**XSGG**	**S4**, **R4**	2316.1	**H13a4**	**A2(1)**, **A2(2)**, **A2(3)**
1097.3	**H6a2**	**A2**, **A3**	2418.2	**P2H12a4**	**A1**, **A2(1)**, **A2(2)**, **A2(3)**
1115.3	**XLGG**	**S4**, **R4**	2434.2	**H14a3**	**A2(2)**, **A2(3)**
1127.4	**XSGGa1**	**A1**, **A2(2)**, **A2(3)**	2448.2	**P1H13a4**	**A2(1)**, **A2(2)**, **A2(3)**
1139.4	**H6a3**	**A3**	2478.2	**H14a4**	**A2(2)**, **A2(3)**
1157.4	**XLGGa1**	**A1**, **A2(2)**, **A2(3)**	2520.3	**H14a5**	**A2(2)**, **A2(3)**
1175.4	**H7**	**A3**	2580.4	**P2H13a4**	**A2(1)**, **A2(2)**
1217.5	**H7a1**	**A2(2)**, **A2(3)**, **A3**			
1247.3	**LSGG**	**S4**, **R4**			
1259.5	**H7a2**	**A2**, **A3**			

[a] m/z of the $[M+Na]^+$ ion.
[b] Nomenclature is as described in the text.

xyloglucan (XyG) and galactoglucomannan (GgM). S2 contained also 27 dw% of the **R1** uronic acid content released from residual pectic polysaccharides or/and from glucuronoxylans (GuX). The bulk of glucose (84 dw% of **R1** glucose) was recovered in the corresponding residue (**R2**) and was attributed essentially to cellulose. **R2** also contained uronic acids, galactose and arabinose (7, 10 and 4 dw%, respectively) together with 2% xylose which evidenced the presence of pectic polysaccharides and residual XyG and/or GuX. **R2** was successively treated with 1.0 and 4.0 M KOH solutions to extract these residual non-cellulosic polysaccharides. The 1 M KOH-soluble fraction (**S3**, 5 dw% from AIM) was composed of about 35% proteins and 27% sugars. The latter were mainly galactose and arabinose (13 and 4 dw%, respectively), probably arising from arabinogalactan-protein (AGP). The 4.0 M KOH extract (**S4**, 6 dw% from AIM) contained less than 1% protein and 67% sugars. The latter were mainly composed of glucose, xylose, galactose and arabinose with a low amount of uronic acids. These were attributed to XyG tightly associated to cellulose together with some remaining AGP and pectins. The material non-accounted for were attributed to ashes due to incomplete dialysis of salts. To summarize, LiCl–DMSO extraction solubilized XyG, GgM pectin and likely GuX. The yield of mannose showed that about 26% of the initial AIM mannose was recovered in the LiCl–DMSO soluble fraction. Such recovery indicate that part of the mannan containing polysaccharides is lost during the extration process and/or tightly associated (linked or intertwinned) with other cell wall structures (Prakash et al., 2012). Further loss (about 13 dw% of AIM) are also observed with KOH extractions that can be attributed in part to protein degradations and incomplete recovery of polysaccharides in extracts.

S2 was fractionated by a DEAE anion-exchange chromatography to separate co-extracted pectin from hemicellulose (Fig. 2A). The latter, recovered in the neutral fraction (**A**), represented 40 dw% of **S2**. It was composed of 44, 24 and 11% of glucose, mannose and xylose, respectively (Table 1) with, galactose and arabinose (16 and 4%, respectively). These sugars were attributed to XyG and GgM with their galactose and arabinose containing side chains. The major fraction from the NaCl gradient (**E**), which amount was equivalent to **A**, was mainly composed of uronic acids (76%) together with galactose, arabinose and rhamnose indicating the presence of rhamnogalacturonans. Fraction **D** was essentially made of xylose corresponding to GuX which is a minor tomato hemicellulose (Quemener, Bertrand, Marty, Causse, & Lahaye, 2007). This fraction yielded after enzymatic hydrolysis by an endo-β-(1,4)-D-xylanase a series of uronic acid substituted β-(1 → 4)-D-xylo-oligomers, some acetyl-esterified (Fig. 3). Glucuronoxylan has been reported to be linked to GgM (Prakash et al., 2012). The isolation of the acidic xylan fraction distinct from GgM suggests that it exists under different forms or that the extraction conditions cleaved the GuX-GgM linkage.

The hemicellulose rich fraction **A** yielded three main fractions, **A1**, **A2** and **A3**, by gel permeation chromatography (Fig. 2B). **A3** fraction was recovered after the total volume of the column

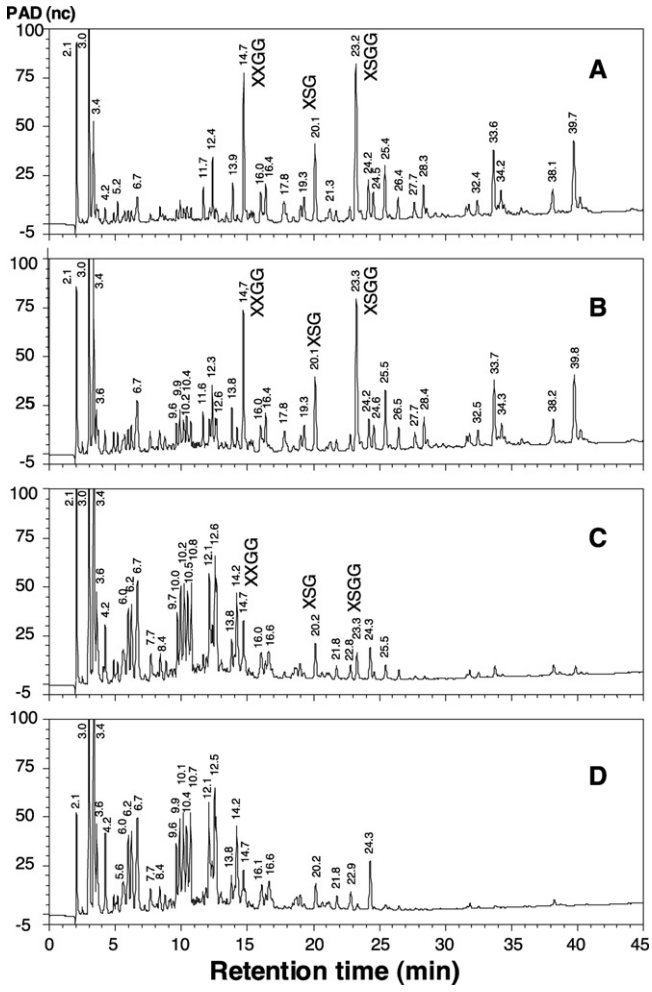

Fig. 6. HPAE chromatogram of β-glucanase degradation products of fractions **A1** (A), **A2(1)** (B), **A2(2)** (C) and **A2(3)** (D).

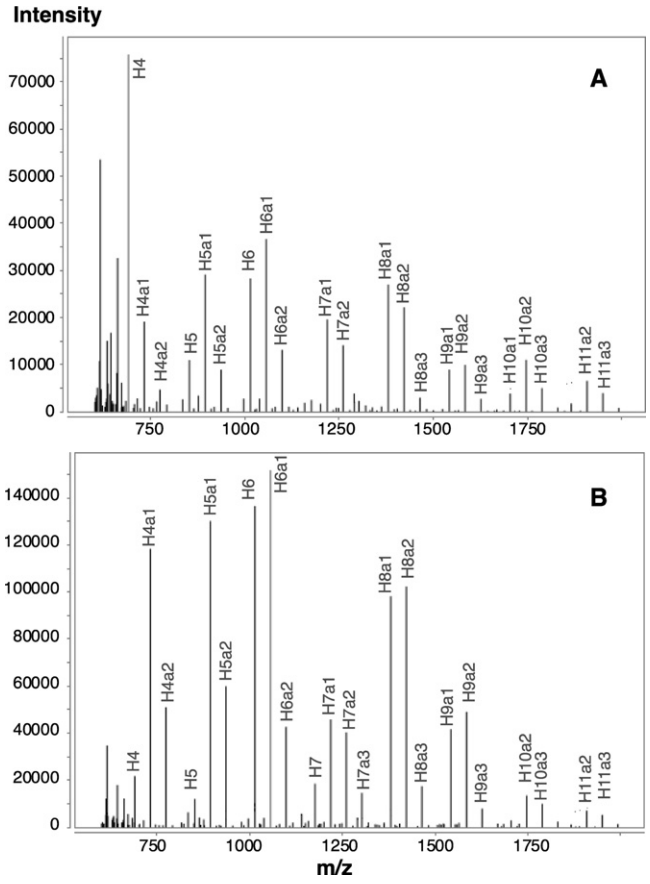

Fig. 7. Mean MALDI-TOF MS spectra of (A) β-glucanase and (B) β-mannase degradation products of **A3** fraction. The nomenclature is as described in the text.

indicating probable hydrophobic interactions between this hemicellulose and the chromatographic phase. The small fraction eluted before fraction **A1** was not retained for further analysis as it represented less than 10% of the initial fraction and was rich in uronic acid. **A1**, **A2** and **A3** represented 17, 43 and 32 dw% of the neutral fraction, respectively. On the basis of sugar composition (Table 1), **A1** appeared principally composed of XyG (50 and 19 dw% of glucose and xylose, respectively), **A2** a combination of XyG and GgM (40, 31, 8 dw% of glucose, mannose and xylose, respectively), and **A3** mainly of GgM (37 and 30 dw% of mannose and glucose, respectively). All three fractions contained galactose (14–15 dw%) and for **A1** and **A2**, arabinose (6 and 2 dw%, respectively). In an attempt to further separate XyG from GgM in **A2**, this fraction was submitted to a second gel permeation chromatography on the same column. Three fractions, **A2(1)**, **A2(2)** and **A2(3)** were obtained (Fig. 3C). **A2(1)** profile elution overlapped the **A1** one and its sugar composition with high xylose and glucose contents and quite poor galactose one (9%) (Table 1) was in support of the presence of XyG. The sugar composition of **A2(2)** and **A2(3)** were close and rich in mannose (about 30%; Table 1), suggesting that GgM was the main component of the two fractions. Their different elution profiles highlighted differences in chemical structures.

Hemicelluloses are usually acetyl esterified (Scheller & Ulvskov, 2010). In order to follow the impact of the LiCl–DMSO extraction on hemicellulose esterification, acetyl esters were quantified in all fractions (Table 1). Acetyl esterification was high in the LiCl–DMSO extract (3.9 dw%), increased in the fraction **A** from anion exchange

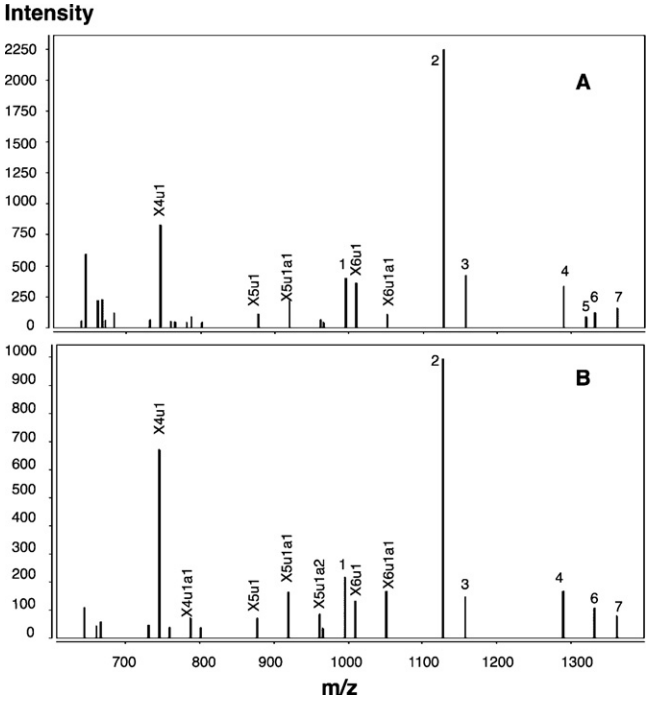

Fig. 8. Mean MALDI-TOF MS spectra of the β-xylanase hydrolyzate of fractions **A2(2)** (A) and **A2(3)** (B) after the second Sephacryl S300 fractionation of **A2**. The nomenclature is as described in the text. Numbers 1 to 7 correspond respectively to **XXGGa1**, **XSGGa1**, **XLGGa1**, **LSGGa1**, **LLGGa1**, **LSGGa2**, **LLGGa2**.

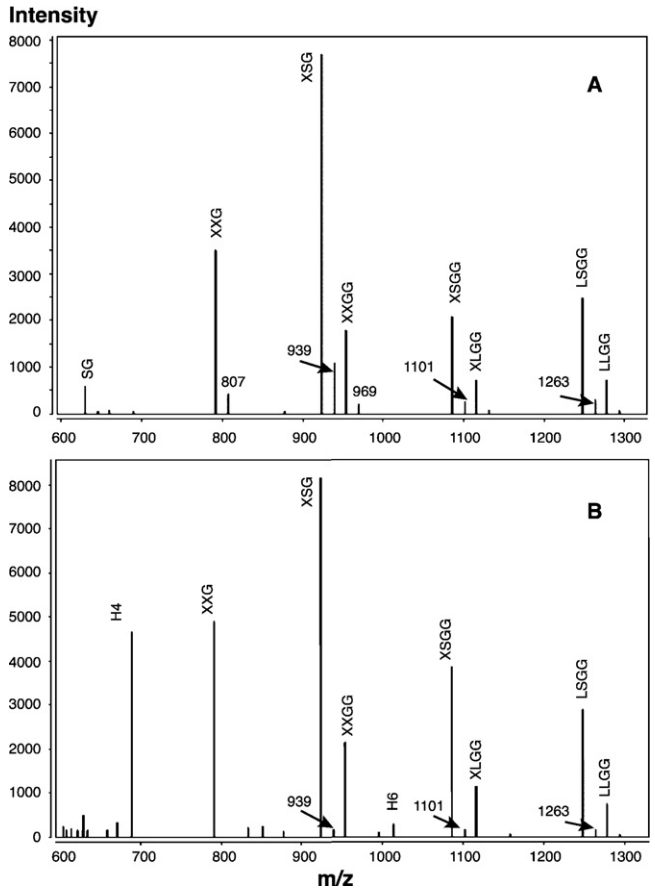

Fig. 9. Mean MALDI-TOF MS spectra of the β-glucanase hydrolyzate of the 4.0 M KOH soluble A) and insoluble B) fractions from the alcohol insoluble residues following pectin, LiCl–DMSO and 1.0 M KOH extractions. The nomenclature is as described in the text.

chromatography (4.3 dw%) and subsequent gel permeation fractions of this fraction (4.5–6.3 dw%). Highest content in acetyl esters were registered for the **A2(2)** and **A2(3)** fractions (6.3 and 6.1 dw%, respectively). These substitutions confirmed the low impact of the LiCl–DMSO solvent on the fine structures of hemicelluloses and the wide occurrence of such esters in all three hemicellulose families.

3.2. Structural analysis of hemicellulose fractions

In order to ascertain the chemical structure of the various fractions obtained after the two successive Sephacryl S300 fractionations, the chromatographic fractions **A1**, **A2**, **A2(1)**, **A2(2)**, **A2(3)** and **A3** were degraded by endo-1,4-β-glucanase, endo-1,4-β-mannanase and endo-1,4-β-xylanase. The oligosaccharides released were analyzed by MALDI-TOF mass spectrometry and HPAEC. The deduced composition and structure of these oligosaccharides are summarized in Table 2.

The MALDI-TOF MS spectra of the β-glucanase degradation products of fractions **A1** and **A2** are shown in Fig. 4. The identification of the peaks released from fraction **A1** (Fig. 4A), on a mass to charge ratio basis, corroborated the presence of mainly xyloglucan oligomers (XyGOs). These were predominantly of the typical Solanacae **XXGG**-type bearing generally one acetyl ester group (Jia et al., 2005; Lahaye et al., 2012; Vincken et al., 1997) but XyGOs of the **XXSG**-type were also observed and were confirmed by ESI-Q-TOF MS of purified oligosaccharides (data not shown). Other minor oligosaccharides corresponded to galactoglucomannan oligomers (GgMOs) such as **H4a1**, **H6a1**, **H11a3**, **H12a4**, **H13a4** and also to a class of hexose oligomers bearing one or two pentosyl residues and four acetyl groups (**P1H12a4**, **P2H12a4** and **P1H13a4**) which intensity increased with that of GgMOs in fraction **A2** (Fig. 4A and B). These shared *m*/*z* with xylosylated and arabinosylated GgM from *Nicotiana* (Sims et al., 1997), and arabinosylated GgM from locust bean gum oligomers (Simões, Nunes, Domingues, & Coimbra, 2011). Considering the low proportion of pentose compared to hexose in this fraction, this series of oligomers was attributed to arabinose or xylose and acetyl substituted GgM structures. The proportion of GgM in **A2** increased as evidenced by acetylated oligomers containing only hexose residues with degree of polymerization varying from 3 to 12. The MALDI-TOF MS spectrum of the β-mannanase degradation products of this fraction corroborated the presence of GgM oligomers though the pentose containing series or smaller oligomers substituted by a pentose unit was absent from the hydrolyzate (Fig. 4C). The different substrate specificities of the glucanase and mannanase proved to be useful in the fine structure characterization of GgM. Structural domains substituted by pentose may not be accessible to mannanase. GgM oligomers released by *A. niger* mannanase are assumed to be composed of alternating glucose and mannose residues with mannose carrying all branched galactosyl units. Moreover, the reducing end mannose may be either unsubstituted or substituted by one galactose residue (Sims et al., 1997). In the light of the high molecular weight oligomers recovered with arabinose or xylose substitution, these likely occurs in region of high substitution of mannose with galactose (galactoside and di-galactoside). Acetyl esterification on the mannose residue can further modulate degradation. The commercial endoglucanase from *Trichoderma longibrachiatum* reported active on konjac glucomannan (Megazyme) remains to be characterized for its substrate specificity with regard to substitution in GgM. In any case, it was able to reveal the presence of block domains with peculiar substitution patterns.

The MALDI-TOF MS spectra of the β-glucanase degradation products of **A2(1)**, **A2(2)** and **A2(3)** obtained after re-fractionation by gel permeation of fraction **A2** are shown on Fig. 5. While the fractions **A2(1)** and **A2(2)** (Fig. 5A and B, respectively) correspond to a mixture of the three classes of populations (XyGOs, GgMOs without and with arabinosyl residues), the fraction **A2(3)** (Fig. 5c) was predominantly composed of GgMOs with low amounts of XyGOs and trace of GgMOs substituted by pentose. The structural composition of β-glucanase degradation products of **A1**, **A2(1)**, **A2(2)** and **A2(3)** was confirmed by HPAEC (Fig. 6). The main peaks eluted at 12.4, 14.7, 20.1 and 23.3 min in Fig. 6A (fraction A1) were collected and analyzed by ESI-Q-TOF mass spectrometry, after a desalting step, for their structural characterization. The respective masses obtained and the MS^2 fragmentation pattern of each purified fraction allowed their identification as **XXG**, **XXGG**, **XSG** and **XSGG** oligomer, respectively (results not shown). In other words, fractions **A1** and **A2(1)** corresponded mainly to xyloglucans. As expected, the proportion of these main XGOS decreased gradually in fraction **A2(2)** and **A2(3)** (Fig. 6C and D). As a consequence, taking account of MALDI-TOF results, the clusters of peaks eluted in the first 12 min of the chromatograms of fraction **A2(1)**, **A2(2)** and **A2(3)** were attributed to oligomers released mainly from galactoglucomannan polymer after glucanase treatment.

The analysis of fraction **A3**, which corresponded to the more retained fraction after the first Sephacryl fractionation, was almost exclusively composed of GgMOs as attested by the MALDI-TOF MS spectra obtained after β-glucanase (Fig. 7A) and β-mannanase (Fig. 7B) treatment. Only some traces of XyGOS were present (**XXG**, **XXGG**, **XXGGa1**, **LSGGa1**, **XTGGa2**, **LLGGa1**).

In order to evaluate the presence of glucuronoxylan in the GgM rich fractions, **A1**, **A2(1–3)** and **A3** were subjected to xylanase degradation and MALDI-TOF MS analyses. Only fractions **A2(2)** and **A2(3)** yielded MS spectra with very low intense ions corresponding to glucuronoxylan oligomers (Fig. 8A and B). These hydrolyzates

also showed xyloglucan oligomers arising from the minor contamination of the commercial xylanase preparation by glucanase.

Extract obtained with 1.0 (**S3**) and 4.0 M KOH (**S4**) as well as the residues after 4.0 M KOH extraction (**R4**) were degraded by glucanase to assess the structure of tightly bound hemicellulose in the cell wall but still accessible to the enzyme. The MALDI-TOF MS profile of the **S3** enzyme digest confirmed the very low hemicellulose content in this fraction (no oligosaccharide detected). Thus, the LiCl–DMSO extract contained hemicellulose usually recovered by 1.0 M KOH. XyGos were detected in **S4** and **R4** (Fig. 9A and B). The oligosaccharide profiles were close and composed of **SGG**, **XXG**, **XSG**, **XXGG**, **XLGG**, **XSGG**, **LSGG** and **LLGG**. They differed by the presence of oligomers of 4 and 6 hexose residues (**H4**, **H6**) in the **R4** profile that can originate from the hydrolysis of cellulose and residual GgM. They also contained a series of ions at *m/z* 807, 939, 969, 1101 and 1263 attributed to the potassium adducts of **XXG**, **XSG**, **XXGG**, **XSGG** and **LSGG** XyGos, respectively. Beside the loss of acetyl esterification, the glucanase oligosaccharide profiles of the 4.0 M KOH soluble and insoluble polysaccharides differed from that of **A1** and **A2** in the LiCl–DMSO extract. In the latter, the structure **XSGGa1** dominated whereas in the alkaline soluble and insoluble XyG, **XSG** was the major ion. These differences support the presence of different XyG populations varying in structural features likely associated with cell wall interactions (Pauly et al., 1999).

4. Conclusions

Acetylated hemicellulose was successfully purified from tomato fruit cell wall by DMSO doped with LiCl, anion exchange and gel permeation chromatography. This procedure allowed the recovery of three distinct families: xyloglucan, galactoglucomannan and glucuronoxylan which structural complexity was conveniently characterized by MALDI-TOF MS and HPAEC after glucanase, mannanase or xylanase degradations. These results provide the first evidence for different distributions of substituants in GgM with respect to pentose (arabinose and/or xylose), some fractions being nearly free of these whereas others being rich in substituted block domains. The glucuronoxylan recovery as an isolated fraction suggests that the GuX-GgM linkage reported in the literature (Prakash et al., 2012) depends on varietal and/or developmental factors or is cleaved during LiCl–DMSO extraction. The LiCl–DMSO soluble hemicellulose likely corresponds to loosely cell wall interacting fraction classically isolated by 1.0 M KOH.

This hemicelluloses extraction procedure open the way for studies aimed at exploring the genetic, developmental and environmental impact on the structural variability of these complex polysaccharide in parenchyma rich plant tissue. In particular, it provides a convenient way to prepare acetylated hemicellulose fractions that will be used for detailed studies on the role of substitutions of these polysaccharides in the cell wall assembly and mechanical properties as well as to serve as original substrates to investigate the details of the cell wall enzymatic structural tailoring during plant development.

Acknowledgments

The authors thank Marie-Jeanne Crépeau (INRA BIA) for technical assistance. Mass spectrometry analyses were performed within the BIBS platform (INRA Centre Angers-Nantes).

References

Abbott, J. A., & Lu, R. (1996). Anisotropic mechanical properties of apples. *Transaction of the American Society of Agricultural Engineers*, *39*, 1451–1459.

Akiyama, Y., Eda, S., & Kato, K. (1984). An acidic xylan from extracellular polysaccharides of suspension-cultured cells of *Nicotiana tabacum*. *Phytochemistry*, *23*, 2061–2062.

Blakeney, A. B., Harris, P. J., Henry, R. J., & Stone, B. A. (1983). A simple and rapid preparation of alditol acetates for monosaccharide analysis. *Carbohydrate Research*, *113*, 291–299.

Blumenkrantz, N., & Asboe-Hansen, G. (1973). New method for quantitative determination of uronic acids. *Analytical Biochemistry*, *54*, 484–489.

Bradford, M. M. (1976). A rapid and sensitive method for the quantitation of microgram quantities of protein utilizing the principle of protein–dye binding. *Analytical Biochemistry*, *72*, 248–254.

Brummell, D. A. (2006). Cell wall disassembly in ripening fruit. *Functional Plant Biology*, *33*, 103–119.

Brummell, D. A., Harpster, M. H., Civello, P. M., Palys, J. M., Bennett, A. B., & Dunsmuir, P. (1999). Modification of expansin protein abundance in tomato fruit alters softening and cell wall polymer metabolism during ripening. *Plant Cell*, *11*, 2203–2216.

Carpita, N. (1984). Fractionation of hemicelluloses from maize cell walls with increasing concentrations of alkali. *Phytochemistry*, *23*, 1089–1093.

Causse, M., Friguet, C., Coiret, C., Lépicier, M., Navez, B., Lee, M., et al. (2010). Consumer preferences for fresh tomato at the European Scale: A common segmentation on taste and firmness. *Journal of Food Science*, *75*, S531–S541.

Chanliaud, E., de Silva, J., Strongitharm, B., Jeronimidis, G., & Gidley, M. J. (2004). Mechanical effects of plants cell wall enzymes on cellulose/xyloglucan composites. *Plant Journal*, *38*, 27–37.

Cosgrove, D., & Jarvis, m. (2012). Comparative structure and biomechanics of plant primary and secondary cell walls. *Frontiers in Plant Science*, *3*, 204.

Cybulska, J., Vanstreels, E., Ho, Q. T., Courtin, C. M., Van Craeyveld, V., Nicolai, B., et al. (2010). Mechanical characteristics of artificial cell walls. *Journal of Food Engineering*, *96*, 287–294.

Dammström, S., Salmén, L., & Gatenholm, P. (2005). The effect of moisture on the dynamical mechanical properties of bacterial cellulose/glucuronoxylan nanocomposites. *Polymer*, *46*, 10364–10371.

Darvill, J. E., McNeil, M., Darvill, A. G., & Albersheim, P. (1980). Structure of plant cell walls. XI. Glucuronoarabinoxylan, a second hemicellulose in the primary cell walls of suspension-cultured sycamore cells. *Plant Physiology*, *66*, 1135–1139.

de Freitas, R. A., Busato, A. P., Mitchell, D. A., & Silveira, J. L. M. (2011). Degalatosylation of xyloglucan: Effect on aggregation and conformation, as determined by time dependent static light scattering, HPSEC-MALLS and viscosimetry. *Carbohydrate Polymers*, *83*, 1636–1642.

Dubois, M., Gilles, K., Hamilton, J., Rebers, P., & Smith, F. (1956). Colorimetric method for the determination of sugars and related substances. *Analytical Chemistry*, *28*, 350–356.

Eda, S., Akiyama, Y., & Kato, K. (1985). A galactoglucomannan from cell walls of suspension-cultured tobacco (*Nicotiana tabacum*) cells. *Carbohydrate Research*, *137*, 173–181.

Eda, S., Akiyama, Y., Kato, K., Takahashi, R., Kusakabe, I., Ishizu, A., et al. (1984). Structural investigation of a galactoglucomannan from cell-walls of tobacco (*Nicotiana-tabacum*) midrib. *Carbohydrate Research*, *131*, 105–118.

Eda, S., Watanabe, F., & Kato, K. (1977). 4-*O*-methylglucuronoxylan isolated from the midrib of *Nicotiana tabacum*. *Agricultural and Biological Chemistry*, *41*, 429–434.

Eklof, J. M., & Brumer, H. (2010). The XTH gene family: An update on enzyme structure, function, and phylogeny in xyloglucan remodeling. *Plant Physiology*, *153*, 456–466.

Flores, M. L., Stortz, C. A., & Cerezo, A. S. (2000). Studies on the skeletal cell wall of the cystocarpic stage of the red seaweed *Iridea undulosa* B. Part II. Fractionation of the cell wall and methylation analysis of the inner core-fibrillar polysaccharides. *International Journal of Biological Macromolecules*, *27*, 21–27.

Frankova, L., & Fry, S. C. (2012). Trans-alpha-xylosidase, a widespread enzyme activity in plants, introduces (1 → 4)-alpha-D-xylobiose side-chains into xyloglucan structures. *Phytochemistry*, *78*, 29–43.

Fry, S. C. (1988). *The growing plant cell wall: Chemical and metabolic analysis*. New York: Longman Scientific and Technical.

Fry, S. C., York, W. S., Albersheim, P., Darvill, A., Hayashi, T., Joseleau, J. P., et al. (1993). An unambiguous nomenclature for xyloglucan-derived oligosaccharides. *Physiologia Plantarum*, *89*, 1–3.

Guillon, F., Philippe, S., Bouchet, B., Devaux, M. F., Frasse, P., Jones, B., et al. (2008). Down-regulation of an auxin response factor in the tomato induces modification of fine pectin structure and tissue architecture. *Journal of Experimental Botany*, *59*, 273–288.

Gunl, M., Neumetzler, L., Kraemer, F., de Souza, A., Schultink, A., Pena, M., et al. (2011). AXY8 encodes an alpha-fucosidase, underscoring the importance of apoplastic metabolism on the fine structure of arabidopsis cell wall polysaccharides. *Plant Cell*, *23*, 4025–4040.

Hagglund, E., Lindberg, B., & McPherson, J. (1956). Dimethylsulphoxide, a solvent for hemicelluloses. *Acta Chemica Scandinavica*, *10*, 1160–1164.

Hoebler, C., Barry, J.-L., David, A., & Delort-Laval, J. (1989). Rapid acid hydrolysis of plant cell wall polysaccharides and simplified quantitative determination of their neutral monosaccharides by gas–liquid chromatography. *Journal of Agricultural and Food Chemistry*, *37*, 360–365.

Jia, Z., Cash, M., Darvill, A. G., & York, W. S. (2005). NMR characterization of endogenously O-acetylated oligosaccharides isolated from tomato (*Lycopersicon esculentum*) xyloglucan. *Carbohydrate Research*, *340*, 1818–1825.

Kalamaki, M. S., Harpster, M. H., Palys, J. M., Labavitch, J. M., Reid, D. S., & Brummell, D. A. (2003). Simultaneous transgenic suppression of LePG and LeExp1 influences rheological properties of juice and concentrates from a processing tomato variety. *Journal of Agricultural and Food Chemistry*, *51*, 7456–7464.

Karas, M., Ehring, H., Nordhoff, E., Stahl, B., Strupat, K., Hillenkamp, F., et al. (1993). Matrix-assisted laser-desorption ionization mass spectrometry with additives to 2,5 dihydroxybenzoic acid. *Organic Mass Spectrometry*, *28*, 1476–1481.

Klee, H. J., & Giovannoni, J. J. (2011). Genetics and control of tomato fruit ripening and quality attributes. *Annual Review Genetics*, *45*, 41–59.

Koubala, B. B., Kansci, G., Mbome, L. I., Crepeau, M. J., Thibault, J. F., & Ralet, M. C. (2008). Effect of extraction conditions on some physicochemical characteristics of pectins from "Amelioree" and "Mango" mango peels. *Food Hydrocolloids*, *22*, 1345–1351.

Lahaye, M., Quemener, B., Causse, M., & Seymour, G. B. (2012). Hemicellulose fine structure is affected differently during ripening of tomato lines with contrasted firmness. *International Journal of Biological Macromolecules*, *51*, 462–470.

Lopez, M., Bizot, H., Chambat, G., Marais, M.-F., Zykwinska, A., Ralet, M.-C., et al. (2010). Enthalpic studies of Xyloglucan–cellulose interactions. *Biomacromolecules*, *11*, 1417–1428.

Lopez, M., Fort, S., Bizot, H., Buleon, A., & Driguez, H. (2012). Chemo-enzymatic synthesis of xylogluco-oligosaccharides and their interactions with cellulose. *Carbohydrate Polymers*, *88*, 185–193.

MacDougall, A. J., Needs, P. W., Rigby, N. M., & Ring, S. G. (1996). Calcium gelation of pectic polysaccharides isolated from unripe tomato fruit. *Carbohydrate Research*, *293*, 235–249.

McCleary, B. V., Gibson, T. S., & Mugford, D. C. (1997). Measurement of total starch in cereal products by amyloglucosidase-α-amylase method: Collaborative study. *Journal of AOAC International*, *80*, 571–579.

Miedes, E., Herbers, K., Sonnewald, U., & Lorences, E. P. (2010). Overexpression of a cell wall enzyme reduces Xyloglucan depolymerization and softening of transgenic tomato fruits. *Journal of Agricultural and Food Chemistry*, *58*, 5708–5713.

Obel, N., Erben, V., Schwartz, T., Kuhnel, S., Fodor, A., & Pauly, M. (2009). Microanalysis of plant cell wall polysaccharides. *Molecular Plant*, *2*, 922–932.

Ordaz-Ortiz, J. J., Marcus, S. E., & Knox, J. P. (2009). Cell wall microstructure analysis implicates hemicellulose polysaccharides in cell adhesion in tomato fruit pericarp parenchyma. *Molecular Plant*, *2*, 910–921.

Park, Y. B., & Cosgrove, D. J. (2012). A revised architecture of primary cell walls based on biomechanical changes induced by substrate-specific endoglucanases. *Plant Physiology*, *158*, 1933–1943.

Pauly, M., Albersheim, P., Darvill, A., & York, W. S. (1999). Molecular domains of the cellulose/xyloglucan network in the cell walls of higher plants. *Plant Journal*, *20*, 629–639.

Pauly, M., Qin, Q., Greene, H., Albersheim, P., Darvill, A., & York, W. S. (2001). Changes in the structure of xyloglucan during cell elongation. *Planta*, *212*, 842–850.

Petruš, L., Gray, D. G., & BeMiller, J. N. (1995). Homogeneous alkylation of cellulose in lithium chloride/dimethyl sulfoxide solvent with dimsyl sodium activation. A proposal for the mechanism of cellulose dissolution in LiCl/Me2SO. *Carbohydrate Research*, *268*, 319–323.

Powell, A. L. T., Kalamaki, M. S., Kurien, P. A., Gurrieri, S., & Bennett, A. B. (2003). Simultaneous transgenic suppression of LePG and LeEXP1 influences fruit texture and juice viscosity in a fresh market tomato variety. *Journal of Agricultural and Food Chemistry*, *51*, 7450–7455.

Prakash, R., Johnston, S. L., Boldingh, H. L., Redgwell, R. J., Atkinson, R. G., Melton, L. D., et al. (2012). Mannans in tomato fruit are not depolymerized during ripening despite the presence of endo-beta-mannanase. *Journal of Plant Physiology*, *169*, 1125–1133.

Quemener, B., Bertrand, D., Marty, M., Causse, M., & Lahaye, M. (2007). Fast data preprocessing for chromatographic fingerprints of tomato cell wall polysaccharides using chemometric methods. *Journal of Chromatography A*, *1141*, 41–49.

Saladie, M., Matas, A. J., Isaacson, T., Jenks, M. A., Goodwin, S. M., Niklas, K. J., et al. (2007). A reevaluation of the key factors that influence tomato fruit softening and integrity. *Plant Physiology*, *144*, 1012–1028.

Sampedro, J., Gianzo, C., Iglesias, N., Guitian, E., Revilla, G., & Zarra, I. (2012). AtBGAL10 is the main Xyloglucan beta-galactosidase in arabidopsis, and its absence results in unusual xyloglucan subunits and growth defects. *Plant Physiology*, *158*, 1146–1157.

Scheller, H. V., & Ulvskov, P. (2010). Hemicelluloses. *Annual Review of Plant Biology*, *61*, 263–289.

Schröder, R., Atkinson, R. G., & Redgwell, R. (2009). Re-interpreting the role of endo-b-mannanases as mannan endotransglycosylase/hydrolases in the plant cell wall. *Annals of Botany*, *104*, 197–204.

Seymour, G. B., Colquhoun, I. J., Dupont, M. S., Parsley, K. R., & Selvendran, R. R. (1990). Composition and structural features of cell-wall polysaccharides from tomato fruits. *Phytochemistry*, *29*, 725–731.

Simões, J., Nunes, F. M., Domingues, M. R., & Coimbra, M. A. (2011). Demonstration of the presence of acetylation and arabinose branching as structural features of locust bean gum galactomannans. *Carbohydrate Polymers*, *86*, 1476–1483.

Sims, I. M., Craik, D. J., & Bacic, A. (1997). Structural characterisation of galactoglucomannan secreted by suspension-cultured cells of *Nicotiana plumbaginifolia*. *Carbohydrate Research*, *303*, 79–92.

Spadiut, O., Ibatullin, F. M., Peart, J., Gullfot, F., Martinez-Fleites, C., Ruda, M., et al. (2011). Building custom polysaccharides in vitro with an efficient, broad-specificity Xyloglucan glycosynthase and a fucosyltransferase. *Journal of the American Chemical Society*, *133*, 10892–10900.

Tokoh, C., Takabe, K., Sugiyama, J., & Fujita, M. (2002). Cellulose synthesized by *Acetobacter xylinum* in the presence of plant cell wall polysaccharides. *Cellulose*, *9*, 65–74.

Tollier, M. T., & Robin, J. P. (1979). Adapation de la méthode à l'orcinol-sulfurique au dosage automatique des glucides neutres totaux: Conditions d'application aux extraits d'origine végétale. *Annales de Technologie agricole*, *28*, 1–15.

Vincken, J.-P., York, W. S., Beldman, G., & Voragen, A. G. J. (1997). Two general branching patterns of xyloglucan, XXXG and XXGG. *Plant Physiology*, *114*, 9–13.

Waldron, K. W., Park, M. L., & Smith, A. C. (2003). Plant cell walls and food quality. *Comprehensive Reviews in Food Science and Food Safety*, *2*, 101–119.